Effect of vacancies on the structural and relaxor properties of $(Sr,Ba,Na)Nb_2O_6$

Anatolii Belous, Oleg V'yunov,[a] and Dmitrii Mishchuk
Vernadskii Institute of General and Inorganic Chemistry, 32/34 Palladina Avenue, 03680 Kyiv, Ukraine

Stanislav Kamba and Dmitry Nuzhnyy
Institute of Physics, Academy of Sciences of the Czech Republic, Na Slovance 2, 18221 Prague 8, Czech Republic

(Received 6 February 2007; accepted 29 May 2007; published online 12 July 2007)

It has been shown that the aliovalent substitution of sodium ions for strontium or barium ions in strontium barium niobate relaxor ferroelectric causes a decrease in vacancy content of the samples and a linear variation of unit cell volume with sodium concentration. The variation of c lattice parameter with sodium concentration is determined by deformations of the NbO_6 oxygen octahedrons in the 001 direction. Dielectric studies carried out in a wide frequency range showed that the decrease in the vacancy content of the $Sr_{0.6-x}Ba_{0.4}Na_{2x}Nb_2O_6$ and $Sr_{0.6}Ba_{0.4-y}Na_{2y}Nb_2O_6$ results in suppression of relaxor ferroelectric properties, which was manifested in both low-frequency and submillimeter region. Simultaneously, rise of the ferroelectric phase transition temperature was observed with increasing sodium concentration. © *2007 American Institute of Physics*. [DOI: 10.1063/1.2752551]

I. INTRODUCTION

The solid solutions $Sr_nBa_{1-n}Nb_2O_6$ (SBN) are formed in the concentration range of $0.2 \leqslant n \leqslant 0.8$ and have a structure of so-called unfilled tetragonal tungsten bronze (TTB).[1,2] The SBN unit cell can be described by the general structural formula $[(A1)_2(A2)_4C_4][(B1)_2(B2)_8]O_{30}$, where $A1$ is the 12-coordinate site situated in the tetragonal structural channels (in the ab plane), $A2$ is the 15-coordinate site situated in pentagonal channels, and C is the 9-coordinate site situated in the triangular channels, which are vacant for SBN. A peculiarity of SBN structure is the distribution of strontium and barium ions between two partially vacant sites $A1$ and $A2$. The tetragonal $A1$ site is occupied by strontium ions only, whereas the pentagonal $A2$ site is statistically filled by the remaining strontium and barium ions. The degree of A-site ion disordering in the two crystallographic sites controls the electrophysical properties of SBN, in particular, the relaxor nature of the temperature dependence of permittivity $\varepsilon(T)$.[3,4] Increasing the [Sr]/[Ba] ratio in SBN shifts the temperature of phase transition in the direction of lower temperatures, increases the permittivity, and enhances the relaxor properties of SBN, which manifest itself by a shift of the temperature of dielectric permittivity maximum with increasing frequency.[1,5] It should be noted that regardless of the [Sr]/[Ba] ratio, 1/6 of the A sites in the SBN structure is empty.

Vacancies and chemical disorder of Sr/Ba cations in the A sites of crystal lattice give rise to the creation of strong dielectric relaxation, which is responsible for the relaxor ferroelectric behavior in SBN.[6] Recent broadband and terahertz spectroscopy investigations[7,8] of SBN confirmed that the dielectric relaxation at 500 K has relaxation frequency in the terahertz range just below the phonon frequencies. The relaxation slows down and broadens on cooling, and finally it splits into two components. The high-frequency one remains in the microwave range, while the low-frequency one is responsible for the dielectric anomaly near T_C: it slows down on cooling and extremely broadens below T_C. At the same time, no phonon anomalies were observed near T_C, which gives evidence about the order-disorder mechanism of the phase transition in SBN.[7]

The partial aliovalent substitution of alkaline ions (for example, sodium) for Sr and Ba ions is one of the possibilities to control the concentration of vacancies in tetra- and pentagonal channels. The electroneutrality condition requires substitution of two Na ions for one Sr or Ba ion, which allows one to control the concentration of vacancies in the A sites.

Therefore, the goal of this work was to study the effect of partial aliovalent substitution of sodium ions for strontium or barium ions on the structure and relaxor properties of strontium barium niobates with the tetragonal tungsten bronze structure.

II. EXPERIMENTAL METHODS

Two systems of solid solutions were investigated in the work: $Sr_{0.6-x}Ba_{0.4}Na_{2x}Nb_2O_6$ $(0 \leqslant 2x \leqslant 0.3)$ and $Sr_{0.6}Ba_{0.4-y}Na_{2y}Nb_2O_6$ $(0 \leqslant 2y \leqslant 0.2)$. Extra pure Nb_2O_5, $BaCO_3$, $SrCO_3$, and Na_2CO_3 were used as starting reagents. After heat treatment of Nb_2O_5 at 850 °C, $BaCO_3$ and $SrCO_3$ at 400 °C, and Na_2CO_3 at 200 °C, required amounts of reagents were weighed using a VLP-200 balance, mixed and homogenized using a GKML-16 vibrating mill (Hungary). Agate drums, chalcedony balls, and acetone as dispersed liquid were used during milling. Thermal analysis was carried out using a Q-1000 derivatograph (MOM Co., Orion, Hungary). Materials were synthesized at 1100–1200 °C, re-

[a]Electronic mail: vyunov@ionc.kar.net

ground in water, dried, and homogenized. A plasticizer was added to the powders, which were then pressed into disks and sintered in a temperature range of 1300–1350 °C.

X-ray powder diffraction (XRPD) data were collected on a DRON-4-07 diffractometer (Cu $K\alpha$ radiation, 40 kV, 20 mA). The structure parameters were refined by the Rietveld full-profile analysis. XRD patterns were collected in the range $2\Theta=10-150°$ in step-scan mode with a step size of $\Delta 2\Theta=0.02°$ and a counting time of 10 s per data point. As external standards, we used SiO_2 (2Θ standard) and Al_2O_3 (NIST SRM1976 intensity standard[9]).

Permittivity ε and dielectric losses tan δ, were measured in a range from 10^5 to 10^6 Hz using a Tesla BM560 Q meter and at 10^9 Hz using the coaxial line method. For measurement we used the cylindrical samples, 2 mm in diameter and 2 mm in thickness. The electrodes were made from silver paste by firing.

Measurements at terahertz frequencies from 3 to 30 cm^{-1} (0.09–0.9 THz) were performed in the transmission mode using a time-domain terahertz spectrometer based on an amplified femtosecond laser system. Two ZnTe crystal plates were used to generate (by optic rectification) and to detect (by electro-optic sampling) the terahertz pulses. Both the transmitted field amplitude and phase shift were simultaneously measured; this allowed us to determine directly the complex dielectric response $\varepsilon^*(\omega)=\varepsilon(\omega)-i\varepsilon''(\omega)$. For sample heating up to 900 K, we used an adapted commercial high-temperature cell (SPECAC P/N 5850) with 1 mm thick sapphire windows.

III. RESULTS AND DISCUSSION

The phase changes occurring during the synthesis of $Sr_{0.6-x}Ba_{0.4}Na_{2x}Nb_2O_6$ and $Sr_{0.6}Ba_{0.4-y}Na_{2y}Nb_2O_6$ systems by solid-state reaction technique were studied for $2x\{2y\}=0.2$, which corresponds to the solid solutions $Sr_{0.5}Ba_{0.4}Na_{0.2}Nb_2O_6$ and $Sr_{0.6}Ba_{0.3}Na_{0.2}Nb_2O_6$. XRPD and thermal analysis showed that the product is formed via the following intermediate compounds: $NaNbO_3$, $Ba_5Nb_4O_{15}$, $Sr_5Nb_4O_{15}$, $BaNb_2O_6$, $SrNb_2O_6$, and $Ba_2NaNb_5O_{15}$. This information allowed us to optimize the synthesis conditions using $NaNbO_3$, $BaNb_2O_6$, and $SrNb_2O_6$ as solid-state precursors. The investigations enabled us to conclude that the solid solutions $Sr_{0.6-x}Ba_{0.4}Na_{2x}Nb_2O_6$ and $Sr_{0.6}Ba_{0.4-x}Na_{2x}Nb_2O_6$ with TTB structure and space group $Pb4m$ are formed in a wide range of x values. When the sodium content is increased $[2x(2y)\geqslant 0.3]$, an additional phase Na_3NbO_4 appears.

The structural parameters of polycrystalline samples of the $Sr_{0.6-x}Ba_{0.4}Na_{2x}Nb_2O_6$ system are listed in Tables I and II. The ion positions of the $Sr_{0.61}Ba_{0.39}Nb_2O_6$ structure, which were reported in Ref. 10, were used as initial values.

The unit cell parameters of the solid solutions $Sr_{0.6-x}Ba_{0.4}Na_{2x}Nb_2O_6$ and $Sr_{0.6}Ba_{0.4-y}Na_{2y}Nb_2O_6$ as a function of sodium content are shown in Fig. 1. The unit cell volume of the solid solutions $Sr_{0.6-x}Ba_{0.4}Na_{2x}Nb_2O_6$ and $Sr_{0.6}Ba_{0.4-y}Na_{2y}Nb_2O_6$ varies linearly with sodium content and obeys Vegard's law. With increasing sodium content, the a parameter decreases in both systems, while the c parameter decreases in the $Sr_{0.6}Ba_{0.4-y}Na_{2y}Nb_2O_6$ system and increases in the $Sr_{0.6-x}Ba_{0.4}Na_{2x}Nb_2O_6$ system.

The a parameter decreases due to a decrease in the average ionic radius $\bar{R}$ in pentagonal channels ($\bar{R}=\alpha R_{Sr}+\beta R_{Ba}$, where α and β are the molar fractions of Sr and Ba, respectively). In the systems $Sr_{0.6-x}Ba_{0.4}Na_{2x}Nb_2O_6$ and $Sr_{0.6}Ba_{0.4-y}Na_{2y}Nb_2O_6$, this decrease occurs due to a decrease in the $4c$-site occupation by strontium and barium, respectively (see Tables I and II). In the system $Sr_{0.6-x}Ba_{0.4}Na_{2x}Nb_2O_6$, the c parameter increases due to the elongation of the NbO_6 oxygen octahedrons in the [001] direction (see Table I), which is accompanied by Nb displacement from the centrosymmetrical position in the oxygen octahedron and by an increase in the acentricity of NbO_6 octahedrons.[2] In the $Sr_{0.6}Ba_{0.4-y}Na_{2y}Nb_2O_6$ system, in contrast to $Sr_{0.6-x}Ba_{0.4}Na_{2x}Nb_2O_6$, the c parameter decreases due to the reduced elongation of oxygen octahedrons in the 001 direction and lower acentricity of the NbO_6 octahedrons (see Table II).

The increase of sodium content from $2x(2y)=0$ to $2x(2y)=0.2$ results in the redistribution of site occupation in the tetragonal and pentagonal channels: namely, the occupation of the double sites in the tetragonal channels increases from 0.71 to 1.15 (1.02), while the occupation of the fourfold sites in the pentagonal channels decreases from 0.89 to 0.79 (0.86) (see Tables I and II). The comparison of our experimental and calculated values of site occupancy in the tetragonal and pentagonal channels allows the conclusion to be drawn that sodium enters the tetragonal channels and that positive charge is compensated in the pentagonal channels by the decrease in strontium (barium) content.

Dielectric characteristics of $Sr_{0.6-x}Ba_{0.4}Na_{2x}Nb_2O_6$ and $Sr_{0.6}Ba_{0.4-y}Na_{2y}Nb_2O_6$ (ε, tan δ) in the frequency range of 10^5-10^9 Hz are shown in Fig. 2. The composition without sodium, $Sr_{0.6}Ba_{0.4}Nb_2O_6$ $[2x(2y)=0]$, is characterized by a considerable relaxation of permittivity (Fig. 2). In this case, the maximum of permittivity ε_{max} shifts by 30 K in the frequency range studied. Regardless of whether barium or strontium ions are substituted, the frequency shift in $\varepsilon_{max}(T)$ decreases with the increase in the sodium content due to the decrease in the A-site vacancy content. One can see that the cation vacancy content has larger influence on the relaxor properties than the [Sr]/[Ba] ratio, which was investigated in Refs. 3 and 4. It is clear from Fig. 2 that the decrease in the cation vacancy content is accompanied by a reduction of the relaxor ferroelectric properties. Temperature of ε_{max} is no more frequency dependent for $2x=0.2$ (or $2y=0.1$), only the values of ε_{max} decrease with increasing frequency, which is typical for diffuse or order-disorder phase transitions, where the relaxation frequency lies slightly above the measured frequency range. The Ba substitution with Na has stronger influence on the suppression of relaxor properties than Sr substitution because the concentration $2y=0.1$ has the same influence on ΔT_{max} as $2x=0.2$.

We fitted the frequencies f and temperatures T_m of the permittivity maxima in Fig. 2 using the Vogel-Fulcher equation,[11]

TABLE I. Crystallographic parameters of samples of the $Sr_{0.6-x}Ba_{0.4}Na_{2x}Nb_2O_6$ system.

	$Sr_{0.6}Ba_{0.4}Nb_2O_6$[a]	$Sr_{0.57}Ba_{0.4}Na_{0.06}Nb_2O_6$	$Sr_{0.55}Ba_{0.4}Na_{0.1}Nb_2O_6$	$Sr_{0.5}Ba_{0.4}Na_{0.2}Nb_2O_6$
	Unit cell parameters [space group *P4bm* (100), $Z=10$]			
a (Å)	12.4566(9)	12.4521(2)	12.4489(2)	12.4417(2)
c (Å)	7.8698(6)	7.8712(1)	7.8734(2)	7.8786(2)
V (Å^3)	1221.1(2)	1220.47(3)	1220.18(4)	1219.57(4)
$P_{x\ ray}$ (g/cm^3)	5.286(1)	5.272(1)	5.262(2)	5.236(2)
	Ion positions			
Nb_1 (2*b*):[b] z/c	0.002 68(19)	0.005(4)	0.010(6)	0.010(5)
Nb_2 (8*d*): x/a	0.074 51(3)	0.0741(1)	0.0736(2)	0.0750(2)
y/b	0.211 61(3)	0.2115(1)	0.2115(2)	0.2111(2)
z/c	−0.007 08(17)	−0.010(9)	−0.010(8)	−0.010(8)
Na/Sr_1 (2*a*):[b] z/c	0.238 2(2)	0.245(4)	0.240(4)	0.263(4)
Ba/Sr_2 (4*c*): x/a	0.172 27(3)	0.1621(4)	0.1611(5)	0.1603(6)
y/b	0.672 27(3)	0.6847(4)	0.6850(5)	0.6836(6)
z/c	0.240 93	0.225(4)	0.251(8)	0.250(4)
O_1 (8*d*): x/a	0.217 9(3)	0.2203(9)	0.226(1)	0.223(1)
y/b	0.282 1(3)	0.2788(9)	0.273(1)	0.276(1)
z/c	−0.015 0(15)	0.025(4)	0.055(4)	0.069(3)
O_2 (8*d*): x/a	0.138 9(4)	0.139(1)	0.141(1)	0.151(3)
y/b	0.069 5(3)	0.072(2)	0.070(2)	0.077(3)
z/c	−0.025 4(11)	−0.025(5)	−0.025(5)	−0.010(5)
O_3 (2*b*): x/a	−0.006 5(4)	−0.018(2)	−0.006(1)	−0.018(2)
y/b	0.344 1(3)	0.336(3)	0.336(2)	0.348(3)
z/c	0.022 9(14)	0.030(9)	0.025(9)	0.046(3)
O_4 (4*c*):[b] z/c	0.234 0(14)	0.236(4)	0.240(4)	0.240(3)
O_5 (8*d*): x/a	0.083 8(9)	0.081(2)	0.093(2)	0.093(3)
y/b	0.200 5(6)	0.204(2)	0.212(2)	0.221(2)
z/c	0.229 9(9)	0.255(4)	0.256(4)	0.260(3)
	Site occupancies			
	Tetragonal channels (position 2*a*)			
Na	0.00	0.15	0.25	0.50
Sr_1	0.71(5)	0.68(1)	0.67(1)	0.65(2)
	Pentagonal channels (position 4*c*)			
Sr_2	0.450(16)	0.41(1)	0.38(1)	0.30(1)
Ba	0.442(20)	0.487	0.487	0.487
	Agreement factors			
R_B (%)	3.3	7.05	9.59	9.90
R_f (%)	4.5	6.52	8.03	9.11
	Some interionic distances			
Nb_1-O_4 (Å)	1.820(11)	1.818(50)	1.811(57)	1.812(46)
Nb_1-O_4, (Å)	2.114(11)	2.117(50)	2.126(57)	2.127(46)
Nb_2-O_5 (Å)	1.874(7)	1.854(77)	1.862(70)	1.830(67)
Nb_2-O_5, (Å)	2.078(7)	2.090(77)	2.111(70)	2.143(67)
	Acentricity of Nb_1 and Nb_2 octahedra			
$\Delta[Nb_1-O_4]$ (Å)	0.29	0.30	0.31	0.31
$\Delta[Nb_2-O_5]$ (Å)	0.20	0.24	0.25	0.31

[a]The structure parameters were refined for sodium-containing compositions only; for composition without sodium ($x=0$), data from Ref. 10 were taken.
[b]Positions: 2*a* (0 0 *Z*), 2*b* (0 1/2 *Z*), and 4*c* (*X* 1/2+*X* *Z*).

$$f = f_0 \exp\left[\frac{-E_a}{k_B(T_m - T_{VF})}\right], \quad (1)$$

where f_0 is the attempt frequency for an ion jump ($f_0 \approx 10^{13}$ Hz), E_a is the activation energy of permittivity relaxation, k_B is the Boltzmann constant, and T_{VF} means the freezing (Vogel-Fulcher) temperature. Figure 3 shows the so-called Vogel-Fulcher plot of $\ln f(T_m\text{-}T_{VF})$. From the fits we obtained the following parameters for $2x(2y)=0$ ceramic SBN sample: $E_a=0.060\pm0.022$ eV and $T_{VF}=320\pm15$ K.

For the ceramics with $2x=0.1$, we obtained $E_a=0.025\pm0.010$ eV and $T_{VF}=410\pm6$ K. In both cases, f_0 was fixed at 1×10^{13} Hz. It was quite difficult to perform the fit just from three T_m temperatures, but the fitting parameters

TABLE II. Crystallographic parameters of samples of the $Sr_{0.6}Ba_{0.4-y}Na_{2y}Nb_2O_6$ system.

	$Sr_{0.6}Ba_{0.4}Nb_2O_6$[a]	$Sr_{0.6}Ba_{0.35}Na_{0.1}Nb_2O_6$	$Sr_{0.6}Ba_{0.3}Na_{0.2}Nb_2O_6$
Unit cell parameters [space group $P4bm$ (100), $Z=10$]			
a (Å)	12.4566(9)	12.4441(2)	12.4260(2)
c (Å)	7.8698(6)	7.8530(2)	7.8471(2)
V (Å^3)	1221.1(2)	1216.08(4)	1211.64(4)
$P_{x\ ray}$ (g/cm^3)	5.286(1)	5.249(1)	5.202(1)
Ion positions			
Nb_1 (2b):[b] z/c	0.002 68(19)	0.020(4)	0.010(4)
Nb_2 (8d): x/a	0.074 51(3)	0.0743(2)	0.0748(2)
y/b	0.211 61(3)	0.2117(2)	0.2113(1)
z/c	−0.007 08(17)	0.021(4)	0.021(4)
Na/Sr_1 (2a):[b] z/c	0.238 2(2)	0.288(4)	0.272(4)
Ba/Sr_2 (4c): x/a	0.172 27(3)	0.1799(7)	0.1819(5)
y/b	0.672 27(3)	0.6649(7)	0.6642(5)
z/c	0.240 93	0.276(4)	0.264(4)
O_1 (8d): x/a	0.217 9(3)	0.224(1)	0.2226(9)
y/b	0.282 1(3)	0.275(1)	0.2765(9)
z/c	−0.015 0(15)	0.082(5)	0.067(5)
O_2 (8d): x/a	0.138 9(4)	0.137(1)	0.139(1)
y/b	0.069 5(3)	0.070(2)	0.065(2)
z/c	−0.025 4(11)	−0.014(5)	−0.020(5)
O_3 (2b): x/a	−0.006 5(4)	−0.010(1)	−0.011(2)
y/b	0.344 1(3)	0.341(2)	0.346(2)
z/c	0.022 9(14)	0.058(5)	0.057(5)
O_4 (4c):[b] z/c	0.234 0(14)	0.275(5)	0.259(5)
O_5 (8d): x/a	0.083 8(9)	0.073(2)	0.085(2)
y/b	0.200 5(6)	0.207(2)	0.208(2)
z/c	0.229 9(9)	0.265(4)	0.276(4)
Site occupancies			
Tetragonal channels (position 2a)			
Na	0.00	0.250	0.500
Sr_1	0.71(5)	0.59(1)	0.52(1)
Pentagonal channels (position 4c)			
Sr_2	0.450(16)	0.47(1)	0.50(1)
Ba	0.442(20)	0.425	0.363
Agreement factors			
R_B (%)	3.3	6.08	7.90
R_f (%)	4.5	5.82	7.74
Some interionic distances			
Nb_1-O_4 (Å)	1.820(11)	1.924(50)	1.954(50)
Nb_1-O_4, (Å)	2.114(11)	2.003(50)	1.970(50)
Nb_2-O_5 (Å)	1.874(7)	1.917(44)	1.927(44)
Nb_2-O_5 (Å)	2.078(7)	2.011(44)	2.005(44)
Acentricity of Nb_1 and Nb_2 octahedra			
$\Delta[Nb_1-O_4]$ (Å)	0.29	0.08	0.02
$\Delta[Nb_2-O_5]$ (Å)	0.20	0.09	0.08

[a]The structure parameters were refined for sodium-containing compositions only; for composition without sodium ($x=0$), data from Ref. 10 were taken.
[b]Positions: 2a (0 0 Z), 2b (0 1/2 Z), and 4c (X 1/2+X Z).

are quite physically reasonable. One can see that with increasing Na concentration, T_{VF} increases and E_a decreases. It is worth noting that in samples with $2x=0.2$ and with $2y \geqslant 0.1$, there is no shift of T_m with frequency (i.e., the relaxor behavior disappears).

The alkaline ions often make contribution to the low-frequency mechanism of polarization, while in the microwave range their contribution is often insignificant.[12,13] Therefore, we considered it expedient to ascertain whether the decrease in the vacancy content due to introducing sodium ions in TTB structure affects the relaxor properties in the submillimeter wave range (terahertz) or it is a low-frequency effect only. The dielectric properties of samples of the $Sr_{0.6-x}Ba_{0.4}Na_{2x}Nb_2O_6$ system were investigated in the

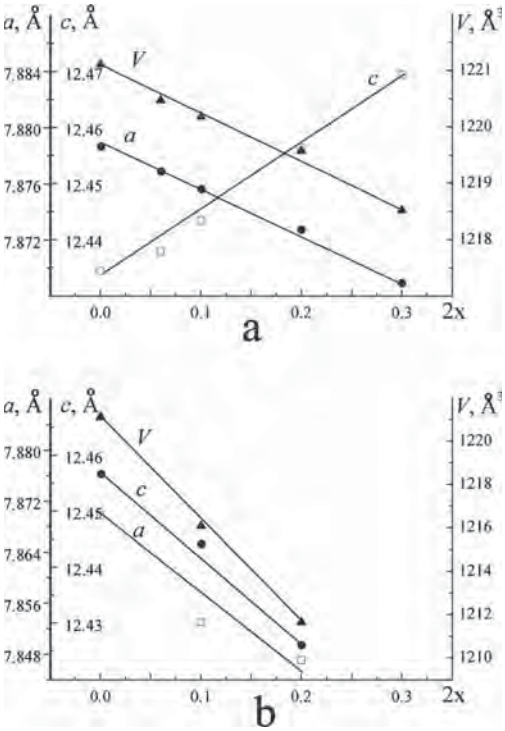

FIG. 1. Unit cell parameters of samples of the $Sr_{0.6-x}Ba_{0.4}Na_{2x}Nb_2O_6$ (a) and $Sr_{0.6}Ba_{0.4-y}Na_{2y}Nb_2O_6$ (b) systems as a function of sodium content.

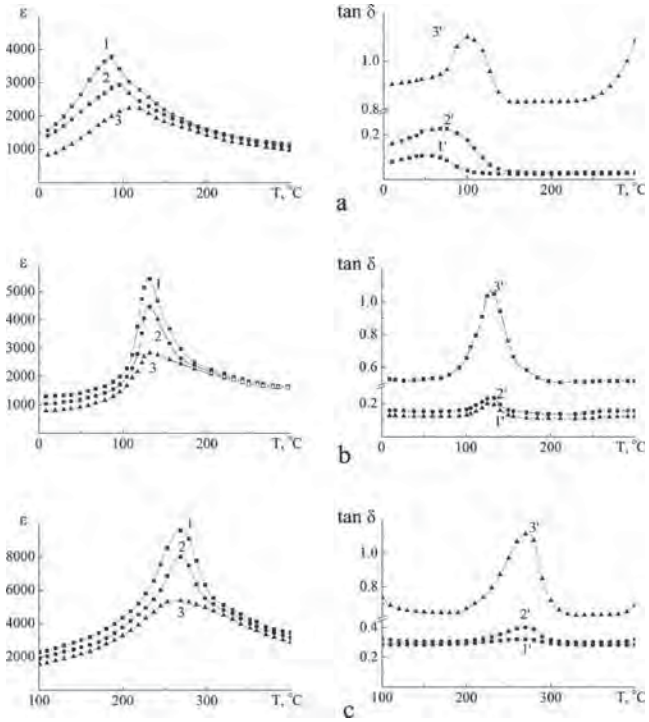

FIG. 2. Permittivity (1–3) and dielectric losses (1′–3′) for samples $Sr_{0.6}Ba_{0.4}Nb_2O_6$, $2x$ ($2y$)=0 (a), $Sr_{0.6}Ba_{0.4-y}Na_{2y}Nb_2O_6$, $2y$=0.1 (b), and $Sr_{0.6-x}Ba_{0.4}Na_{2x}Nb_2O_6$, $2x$=0.2 (c). Values were measured at 10^5 Hz (1,1′), 10^6 Hz (2,2′), and 10^9 Hz (3,3′).

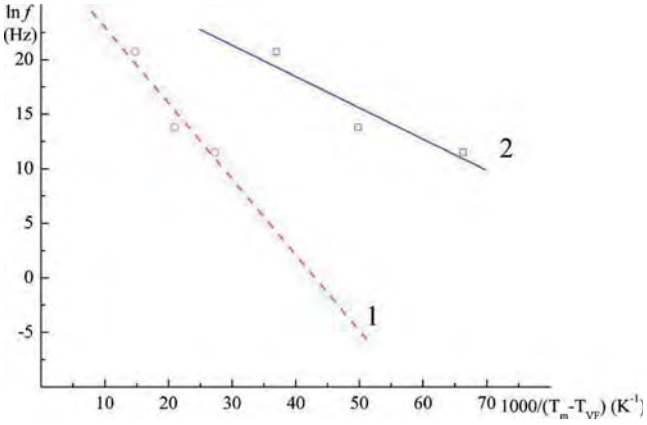

FIG. 3. (Color online) Vogel-Fulcher plots of frequencies and temperatures of the permittivity maxima for the $Sr_{0.6-x}Ba_{0.4}Na_{2x}Nb_2O_6$ system.

terahertz frequency range. Results of these investigations for samples with $2x$=0 and $2x$=0.2 are presented at various temperatures in Figs. 4(a) and 4(b). We have investigated also samples with $2x$=0.06 and $2x$=0.1, but the results are not presented here. Nevertheless, the shape of the spectra is the same for all the sample compositions: permittivity ε decreases with frequency, and dielectric loss ε'' is rather high. This indicates a dielectric relaxation in the terahertz frequency range. Both ε and ε'' increase on heating to T_m or T_C, and then they decrease on further heating. This indicates slowing down of the dielectric relaxation on cooling. The relaxation frequency is above 25 cm^{-1} at 900 K and slows down on reducing temperature to our terahertz frequency range. Below T_m (T_C) the relaxation frequency slows below this range (to microwave or lower frequency range); therefore the terahertz values of both ε and ε'' decrease on cooling below T_m (T_C). The presence of dielectric relaxation manifests an order-disorder type of the phase transitions in all the samples. Low-frequency terahertz permittivity is much higher in the $2x$=0 sample than in the $2x$=0.2 ceramic be-

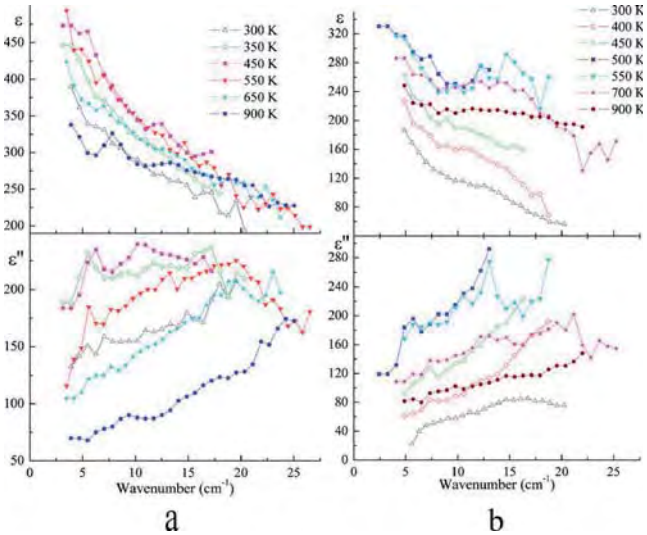

FIG. 4. (Color online) Terahertz complex dielectric spectra of $Sr_{0.6-x}Ba_{0.4}Na_{2x}Nb_2O_6$ ceramics with (a) $2x$=0 and (b) $2x$=0. The open and filled symbols denote temperatures below and above T_C, respectively.

cause the dielectric strength ($\Delta\varepsilon$) of relaxation is much higher in the undoped sample. This indicates that each Sr substitution by 2Na cations reduces the disorder in the crystal lattice due to the reduction of the vacancy concentration.

It is well known that the relaxor ferroelectric behavior (i.e., the shift of permittivity peaks with measured frequency) occurs as a consequence of anomalous broadening of the distribution of relaxation frequencies on cooling.[14,15] This effect in pure SBN was recently experimentally confirmed.[7,8] Na doping of SBN reduces the vacancy concentration and therefore also random fields, which are responsible for the broad distribution of relaxation frequencies in relaxor SBN. Distribution of relaxation frequencies dramatically decreases with Na concentration, and therefore the relaxor ferroelectric behavior disappears in samples with higher Na concentration, and the sample exhibits only classical order-disorder phase transition with critical relaxation starting in the terahertz range (at high temperatures), which slows down to the megahertz range near T_C. It is worth noting that the relaxation remains in the terahertz spectra of SBN up to the highest measured temperature 900 K, while it disappears in lead-based perovskite relaxor ferroelectrics above 600–700 K, i.e., above the Burns temperature (600–700 K), where the polar clusters disappear.[16] It seems to be the only difference between perovskite relaxors and our SBN relaxor system. This is presumably connected with the intrinsic (single particle) disorder in the SBN lattice at high temperatures which produces dielectric relaxations without any need of polar nanoregions. For that reason it might be quite a hard problem to estimate in the SBN the Burns temperature, where the single particle relaxation changes into a collective relaxation of polar nanoregions.

IV. CONCLUSION

It has been found that the formation of the $Sr_{0.6-x}Ba_{0.4}Na_{2x}Nb_2O_6$ and $Sr_{0.6}Ba_{0.4-y}Na_{2y}Nb_2O_6$ solid solutions is a multistage process involving the following intermediate phases: $NaNbO_3$, $Ba_5Nb_4O_{15}$, $Sr_5Nb_4O_{15}$, $BaNb_2O_6$, $SrNb_2O_6$, and $Ba_2NaNb_5O_{15}$. It has been shown that the aliovalent substitution of sodium ions for strontium or barium ions, which is accompanied by a decrease in the vacancy content, causes a linear variation of unit cell volume in the entire x range investigated ($0 \leqslant 2x \leqslant 0.3$). The variation of the c lattice parameter with x is determined by deformations of the NbO_6 oxygen octahedra in the [001] direction. The investigations carried out in a wide frequency range showed that the decrease of the vacancy content in the $Sr_{0.6-x}Ba_{0.4}Na_{2x}Nb_2O_6$ and $Sr_{0.6}Ba_{0.4-x}Na_{2x}Nb_2O_6$ systems due to partial substitution of sodium ions for strontium or barium ions results in suppression of relaxor properties, which is observed both in the low-frequency and submillimeter range. It was also shown that the barium substitution by sodium suppresses the relaxor properties more effectively than in the case of the strontium substitution.

ACKNOWLEDGMENTS

The work has been supported by The Science and Technology Center in Ukraine (Project No. 3898) and the Grant Agency of the Czech Republic (Project No. 202/06/0403). The authors thank J. Petzelt for critical reading of the manuscript.

[1] M.-S. Kim, P. Wang, J.-H. Lee, J.-J. Kim, H. Y. Lee, and S.-H. Cho, Jpn. J. Appl. Phys., Part 1 **41**, 7042 (2002).
[2] T. S. Chernaya, B. A. Maksimov, T. R. Volk, L. I. Ivleva, and V. I. Simonov, Phys. Solid State **42**, 1716 (2000).
[3] L. E. Cross, Ferroelectrics **76**, 241 (1987).
[4] J. R. Oliver, R. R. Neurgaonkar, and L. E. Cross, J. Appl. Phys. **64**, 37 (1988).
[5] J. G. Carrio, Y. P. Mascarenhas, W. Yelon, I. A. Santos, D. Garcia, and J. A. Eiras, Mater. Res. **5**, 57 (2002).
[6] W. Kleemann, J. Dec, P. Lehnen, R. Blinc, B. Zalar, and R. Pankrath, Europhys. Lett. **57**, 14 (2002).
[7] E. Buixaderas, M. Savinov, M. Kempa, S. Veljko, S. Kamba, J. Petzelt, R. Pankrath, and S. Kapphan, J. Phys.: Condens. Matter **17**, 653 (2005).
[8] J. Banys, J. Macutkevic, R. Grigalaitis, and W. Kleemann, Phys. Rev. B **72**, 024106 (2005).
[9] Certificate of Analysis, Standard Reference Material 1976, Instrument Sensitivity Standard for X-ray Powder Diffraction (National Institute of Standards and Technology, Gaithersburg, 1991), p. 4.
[10] T. Woike *et al.*, Acta Crystallogr., Sect. B: Struct. Sci. **59**, 28 (2003).
[11] S. Kamba *et al.*, Phys. Rev. B **66**, 054106 (2002).
[12] A. G. Belous, Theor. Exp. Chem. **34**, 331 (1998).
[13] A. G. Belous, J. Eur. Ceram. Soc. **21**, 2717 (2001).
[14] D. Viehland, M. Wuttig, and L. E. Cross, Ferroelectrics **120**, 71 (1991).
[15] S. Kamba *et al.*, J. Phys.: Condens. Matter **12**, 497 (2000).
[16] V. Bovtun, S. Veljko, S. Kamba, J. Petzelt, S. Vakhrushev, Y. Yakymenko, K. Brinkman, and N. Setter, J. Eur. Ceram. Soc. **26**, 2867 (2006).